Mem. Fac. Eng., Osaka City Univ., Vol. 48, pp. 45–50 (2007)

Mechanical Behavior of Concrete Filled Tube with Large Width-Thickness Ratio of Steel Plate

Hisao Tsunokake*, Yasunori KOBAYASHI** and Hajime OHUCHI***

(Received September 28, 2007)

Synopsis

Present study is to investigate mechanical behavior of concrete filled steel tube members (CFT) with thinner steel plate than specified in considering practical application to either new or strengthening existing members. Asymmetric four-point static loading test have been conducted for beam type specimens with a square cross section. Test parameters were shear-span ratios of 1.0 to 2.0 and steel tube width-thickness ratios of 65 to 200. Three dimensional nonlinear finite element analyses have been also conducted for test results. Flexural mode failure has been observed for shear span ratio of 2 and shear mode failure for that of 1 in good agreement with analytical results respectively.

Key Words: CFT, Large Width-Thickness Ratio, Shear Span Ratio, Composite Member

1. Introduction

Concrete filled steel tube (CFT) member has been widely applied to not only infrastructures but architectural building structures as well due to more advantages in strength and ductility characteristics. Many studies have been actively carried out. However most of them are focusing on the member with small width-thickness ratio or diameter-thickness ratio of steel plate. In the design of infrastructures such as bridges, axial stress-strength ratio is generally less than architectural structure, which means larger cross section dimension employed. Accordingly, larger width-thickness ratio or diameter-thickness ratio employed is considered as rational for structural design of infrastructures. Authors[1],[2] have conducted experimental studies using specimens with larger width-thickness ratio of steel plate. Among of them, Tsunokake etc. [1] have conducted experimental studies on square cross section CFT members with 200 or more in width-thickness ratio, largely beyond the specified range in the architectural building standard [3]. However, the comparative review should be added for wider range of that including specified ranges. In these background, authors have carried out flexural shear loading tests of model specimens with test parameters of shear-span ratio a/d of 1.0 or 2.0 and of width-thickness ratio B/t of 65, specified limited value, and 125 or 200 focusing on nonlinear behavior up to the ultimate loading capacity. Three dimensional finite element nonlinear analyses have been carried out to predict experimental results with modeling not only material nonlinearity in both steel and concrete but bond slip action between both materials as well.

2. Outline of Experiment

Model specimens are of square cross section with 200 mm side length and of span length with 400 or 800mm. No connection is arranged at all inside of the steel tube. End section of steel plate is increased in thickness for buckling prevention and is welded with bearing end plate. As illustrated in Fig.1, load application is asymmetric four-point static loading method so as to uniform shear force applied, where end bearing plate is bolted with side beam. Three kinds of measurement devices are instrumented as shown in the figure. First, five displacement transducers are placed at mid-span, support and loading points to examine deformation property as whole specimen. Second, fifteen tri-axial type strain gauges are attached on both side webs of the tube at mid span to both ends to evaluate elasto-plastic stresses in the web. Last, eight

* Research Associate, Department of Civil Engineering
** West Japan Railway Company
*** Professor, Department of Civil Engineering

uni-axial type strain gauges are also attached on both side flanges to evaluate buckling and elasto-plastic stresses. Test parameters are shear-span ratio i.e. a/d=1.0 and 2.0 and width-thickness ratio, i.e. B/t=62.5 (t=3.2), 125 (t=1.6) and 200 (t=1.0). Table.1 summarizes dimensions of specimens, material properties and estimated strengths. The specimen is named due to nominal thickness as followed by T and shear-span ratio followed by S. Flexural capacity P_m in the table is calculated based on AIJ Standard for Steel Reinforced Concrete Structures [3]. Shear capacity P_s is calculated as the superposed strength of a steel tube and core concrete, where shear capacity of a steel tube is by Design Code for Steel Structures PART B [4] and that of core concrete by considering deep beam action in Standard Specifications for Concrete -Structural Performance [5]. In the case, the steel tube flange is modeled as compression and tension reinforcement.

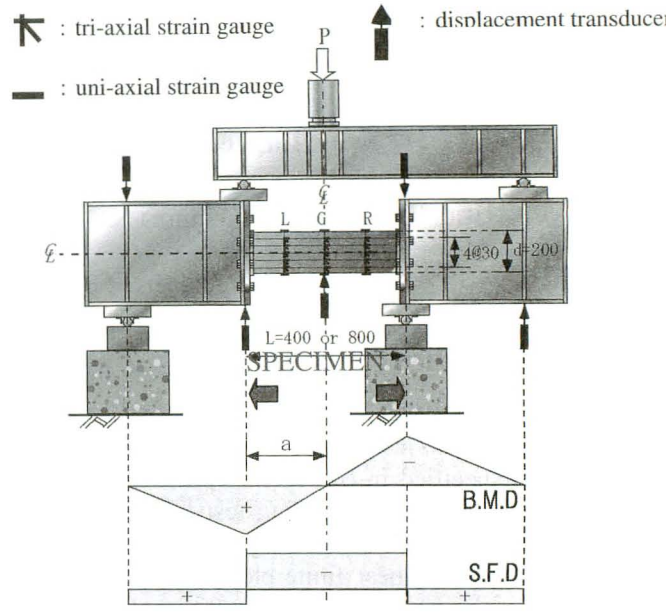

Fig-1 Test Setup and Measurement Devices

Table-1 Summary of Specimens

Tag	Dimensions of specimens						Material properties of steel tube				Material properties of concrete		Estimated strength		Experimental strength
	t_0	t_s	B	B/t_s	a	a/d	σ_{sy}	σ_{sB}	E_s	E_s'	σ_c	E_c	P_m	P_s	P_{max}
	(mm)	(mm)	(mm)		(mm)		(MPa)	(MPa)	(GPa)	(GPa)	(MPa)	(GPa)	(kN)	(kN)	(kN)
T32-S1	3.2	3.10	200	65	200	1	181.6	307.4	195.1	1.82	25.8	25.4	440.3	485.2	661.8
T32-S2	3.2	3.10		65	400	2	181.6	307.4	195.1	1.82	26.4	25.3	264.5	448.9	500.5
T16-S1	1.6	1.57		127	200	1	215.9	335.3	199.5	2.43	25.4	25.4	277.9	347.5	450.5
T16-S2	1.6	1.57		127	400	2	215.9	335.3	199.5	2.43	26.2	25.4	167.0	304.1	302.3
T10-S1	1.0	0.95		210	200	1	209.8	320.7	195.1	2.22	18.9	22.6	167.0	236.7	315.0
T10-S2	1.0	0.95		210	400	2	209.8	320.7	195.1	2.22	25.7	25.4	101.4	211.3	190.0

Note: t_0: nominal thickness; t: measured thickness; B: cross-sectional breadth; a: shear span length; d: effective depth;
For steel tubes, σ_{sy}: yielding point; σ_{sB}: breaking point; E_s: young's modulus; E_s': work hardening coefficient;
For concrete, σ_c: cylindrical strength; E_c: young's modulus;
P_m: flexural strength; P_s: shear strength; P_{max}: maximum experimental strength

3. Experimental Results

3.1 Failure Mode

After the loading test completed, cracking pattern of the filled concrete was observed peeling the tube off as shown in Fig.2. As shown in figure-2 (1), diagonal crack is observed in the mid section of shear-span ratio of one specimens, independent on width-thickness ratio. Yet, as shown in figure-2(1) (b), flexural crack is observed at both ends in the T32-S1 specimen with higher loading capacity. In the shear-span ratio of two specimens with a local buckling occurrence in the compressive flange, some flexural cracks are observed at end section. The smaller width-thickness ratio, more cracks are observed, while as for buckling of steel plate, any difference is not observed at all between T16-S2 and T32-S2 specimens.

In general, number of cracks is more in large width-thickness ratio specimens in both one and two shear-span ratio specimens. As for ultimate failure pattern, shear span ratio of one specimen is categorized as shear failure, while that of two specimen as flexural failure.

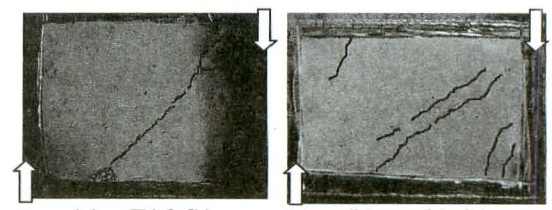

(a) T16-S1 (b) T32-S1

(1) shear-span ratio of one

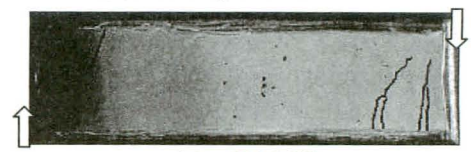

(a) T16-S2

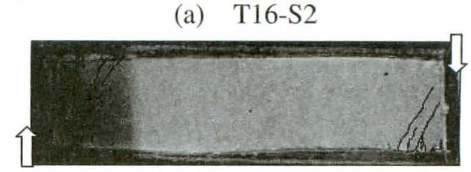

(b) T32-S2

(2) shear-span ratio of two

Fig-2 cracks in core concrete

3.2 Load-Displacement Relationship

Figure 3 shows relationships between normalized load (shear-span ratio 1: load P/P_s and shear-span ratio 2: P/P_m) and drift angle (displacement δ /specimen length L), where circular symbol provides yielding initiation at web section, and triangular that at flange section respectively. In addition, square symbol provides buckling initiation.

In the specimens with shear-span ratio of one, web plate yields at below P/P_s of 0.5 and flange plate yields at P/P_s of 0.5-0.65. It means that shear yielding is significant even in the steel tube. Especially, in the T16-S1 specimen, shear yielding initiates at earlier stage than other specimens and as the results, drift angle at maximum load provides largest value. However, in general, there is no significant difference in maximum load among specimens, which is around 1.3 to 1.4 value, while no co-relationship is found in maximum drift angle dependent on plate width to thickness ratio.

In the specimens with shear-span ratio of two, except T16-S2 specimen, yielding initiates at flange section followed by that at web section. No co-relationship is found in local buckling load among specimens, dependent on plate width to thickness ratio. The smaller the width-thickness ratio, normalized initial stiffness becomes smaller. Among specimens, no significant difference is observed in normalized maximum load which is about 1.8 to 1.9.

4. Finite Element Nonlinear Analysis

Three dimensional finite element nonlinear analyses are conducted with using computer program FINAL. Half model, which is consisted with test specimen and elastic side beam, is analyzed with considering asymmetric geometry as shown in figure 4(a). The modeling of side beam is for consideration of elastic deformation of that. No buckling phenomenon is considered for steel tube.

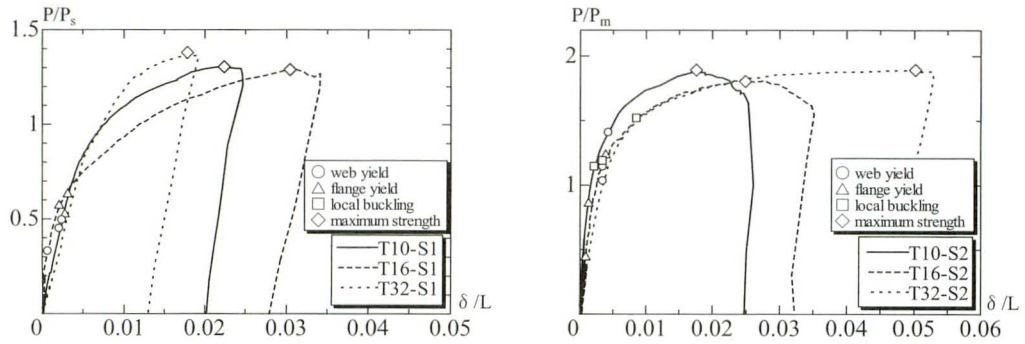

(a) 1.0 of shear-span ratio (b) 2.0 of shear-span ratio

Fig-3 Normalized load – rotation relation

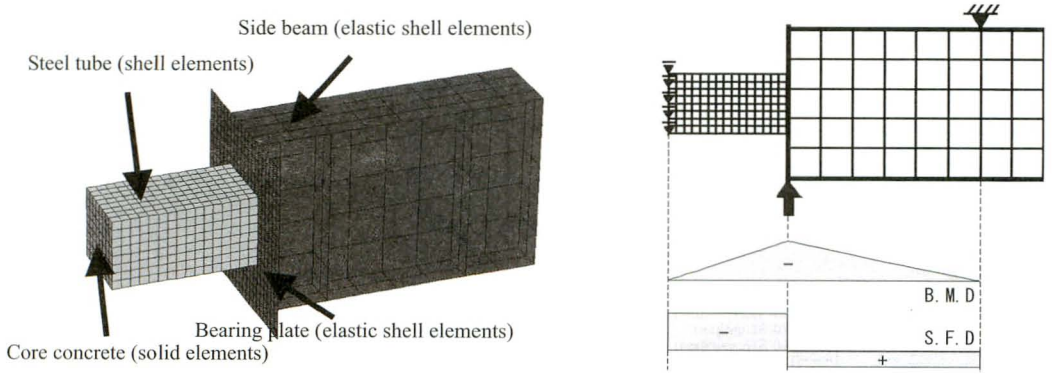

(a) Overall view of idealization (b) Boundary condition

Fig-4 Analytical Model

4.1 Concrete

Filled concrete section is modeled into assembly of solid element. Inelastic constitutive law employed is orthogonal model based on equivalent uni-axial strain. Figure 5(a) shows uni-axial stress-strain relationship, which consists of Modified Ahmad model [6] for ascending part and Izumo model for descending part [6] respectively.

4.2 Steel tube

A steel tube is modeled into assembly of shell elements. Figure 5(b) shows uni-axial stress-strain relationship for steel tube which is modeled by bi-linear relationship. The constitutive law in bi-axial stress state is based on associated flow rule with Von Mises equation as a yield function.

4.3 Interface between Steel and Concrete

The interface between concrete and steel flange or web section is modeled by the joint element with considering bond slip relationship between these materials [7] as shown in figure 5. Furthermore, the interface between concrete and end bearing plate, where possible opening is expected, is modeled by separate nodes.

5. Analytical Result

5.1 Load-Displacement

In figure-7, analytical load-displacement relationships are shown in comparison with experimental results. In the specimen of shear-span ratio of one, analytical initial stiffness is larger than experimental result. However, good agreement is obtained in maximum load capacity between analytical and experimental results among all specimens except T32-S1 specimen in which more difference is obtained in measured displacement at asymmetric point. In the specimen of shear-span ratio of two, good agreement is obtained between both results among all specimens

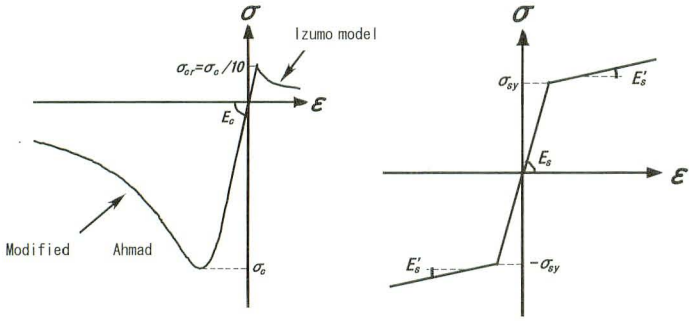

(a) filled concrete (b) steel tube

Fig-5 Stress - strain relationships

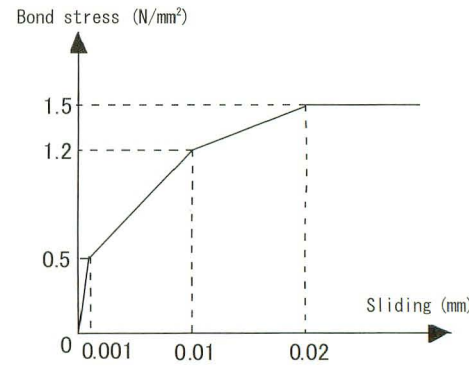

Fig-6 Bond stress – sliding relationships

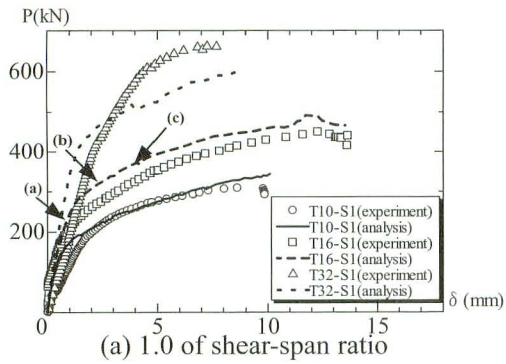

(a) 1.0 of shear-span ratio

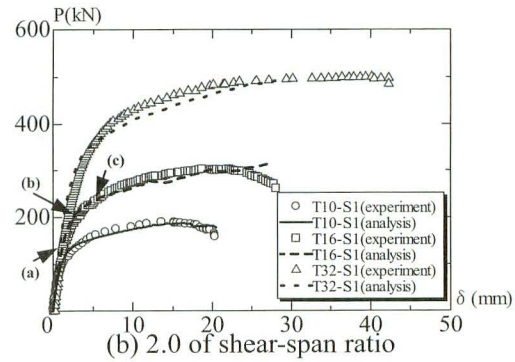

(b) 2.0 of shear-span ratio

Fig-7 load-displacement relationships

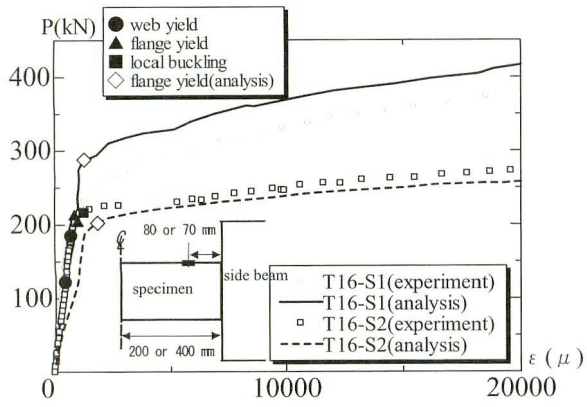

Fig-8 Load-Flange Strain Relationships

5.2 Load- Strain Relationship at Flange Section

Figure-8 represents load strain relationship at tensile flange section of T16 specimen. Analytical results provide good agreement with experimental values for both shear-span ratio of one and two specimens. These good agreements are provided with all 6 specimens. Accordingly, applicability of the present analysis is confirmed.

Based on these good predictions, further discussion is developed focusing on T16-S1 and T16-S2 specimens as representative examples.

5.3 Yielding at Web Section

Analytical Mises stress contour for steel tube web section is provided in fig.9 and10, where Mises stress, σ_{eq} is defined in the following equation.

$$\sigma_{eq}^2 = \sigma_x^2 + \sigma_y^2 - \sigma_x\sigma_y + 3\tau_{xy}^2 \qquad (1)$$

The left end of the figure is mid section of specimen. Experimental Mises stress calculated by measured strain is provided with the circle in the figure. White and black circle provide experimental Mises stresses in elastic and plastic states respectively, where (a) to (c) corresponds to each load level as an arrow in the Fig.6. In the T16-S1 specimen, Mises stress diagonally increases from middle to right end section and yielding region develops more with load increase. In the end section, flexural stress affects more.

On the other hand, in the T16-S2 specimen as shown in Fig.10, Flexural stress affects more on the Mises stress development. Yielding region dominates at the up end section, where flexural tensile stress dominates more.

5.4 Stress Flow

Fig.11 illustrates analytical maximum principal stress flow. In the T16-S1 specimen, these diagonal stresses uniformly distribute, that suggests predominance of shear stress. On the other hand, in the T16-S2 specimen, these stresses horizontally dominate at right end section, that suggests predominance of flexural tensile stress, while less

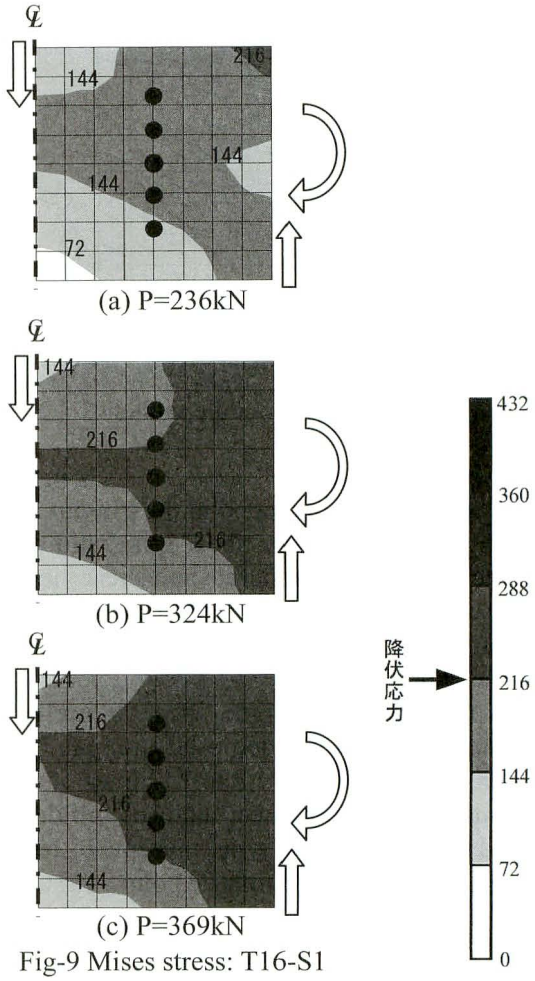

Fig-9 Mises stress: T16-S1

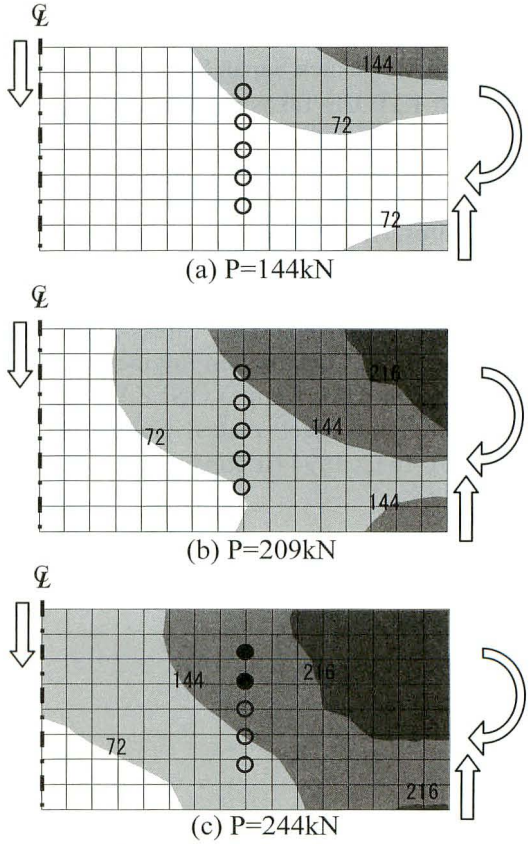

Fig-10 Mises stress: T16-S2

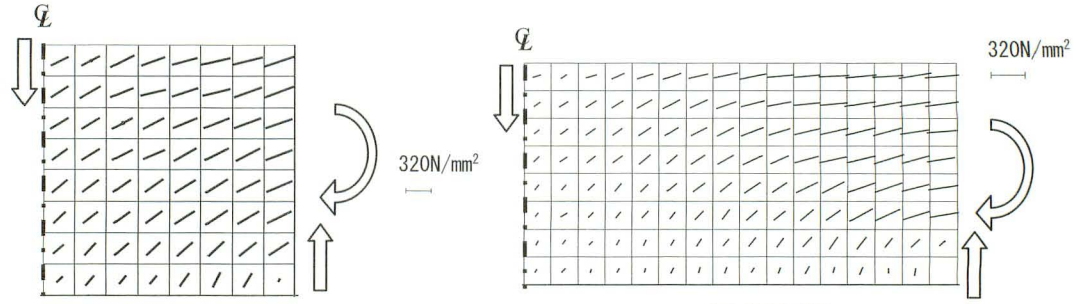

(a) T16-S1 (b) T16-S2

Fig-11 Maximum principal stress

diagonal stress appears at middle section.

6. Concluding Remarks

Followings are concluded in the present study.

1) As for failure pattern, shear-span ratio of one specimen provides shear failure with significant diagonal crack to the filled concrete and shear yielding to the steel tube. On the other hand, shear-span ratio of two specimen provides flexural failure with flexural crack of concrete and local buckling to the end section. Furthermore, number of cracks tends to increase more with decrease of width-thickness ratio of steel tube.
2) As for ultimate strength, shear failure type specimens, i.e. shear-span ratio of one, provide 1.3 to 1.4 times of specified superposed strength. On the other hand, flexural failure type specimens, i.e. shear-span ratio of two, provide 1.8 to 1.9 times of that.
3) Finite element nonlinear analysis provides good agreement with the experimental results for both shear and flexural failure types except T32-S1 specimen, in which some difference obtained in measured displacement at asymmetric point.

7. References

[1] Hisao TSUNOKAKE, Kazumasa WAKISAKA, Keiichiro SONODA, and Harutoshi KOBAYASHI : Basic Study on Shear Capacity of CFT Members with a Large Width-thickness Ratio of Steel Plate, Journal of Applied Mechanics, Japan Society of Civil Engineers (JSCE), Vol.5, pp.377-384, 2002 (in Japanese)

[2] Hiroaki KITOH, Takashi KOYABU, Keisuke SAHARA and Keiichiro SONODA : Concrete Filled Circular Steel Tubular Stubs with a Large Ratio of Diameter to Thickness under Compression, Journal of Structural Mechanics and Earthquake Engineering, JSCE, No. 759, pp.25-36, 2004 (in Japanese)

[3] Architectural Institute of Japan (AIJ) : AIJ Standard for Structural Calculation of Steel Reinforced Concrete Structures, AIJ, 2001 (in Japanese)

[4] JSCE : Design Code for Steel Structures PART B ; Composite Structures, 1997 (in Japanese)

[5] JSCE : Standard Specifications for Concrete –Structural Performance Verification-, 2002 (in Japanese)

[6] Kazuhiro NAGANUMA : Stress-Strain Relationship for Concrete under Triaxial Compression, Journal of Structural and Construction Engineering Transactions of AIJ, AIJ, No. 474, pp.163-170, 1995 (in Japanese)

[7] Kwangyeon KIM, Kenji YONEZAWA, Hiroshi NOGUCHI : Experimental Study on Bond Characteristics of Concrete and Steel plates, Summaries of Technical Papers of Annual Meeting AIJ. Structures II , pp.1631-1632, 1994 (in Japanese)